

Analysis of the anatomic variations of the ethmoid roof among Saudi population: A radiological study

Gisma A. Madani^{1,2}, Abdelmoneim S. El-mardi^{2,3}, Wael Amin Nasr El-Din^{1,4}

¹Anatomy Department, Ibn Sina National College for Medical Studies, Jeddah, Saudi Arabia ²Anatomy Department, Faculty of Medicine, The National University, Khartoum, Sudan ³Anatomy Department, Faculty of Medicine, Almaarefa University, Riyadh, Saudi Arabia ⁴Department of Human Anatomy and Embryology, Faculty of Medicine, Suez Canal University, Ismailia, Egypt

SUMMARY

The olfactory fossa (OF) is a depression in the anterior cranial cavity whose floor is formed by the cribriform plate of ethmoid, bounded laterally by the lateral lamella of cribriform plate and medially by crista galli. Keros categorized the olfactory fossa depth into 3 types. For a successful endoscopic sinus surgery, the surgeons should pay attention to the details when dealing with the complex anatomy of the paranasal sinuses (PNS) and skull base. The aim of this study was to describe the distribution of Keros classification of the height of ethmoid roof among Saudi population by using multidetector computed tomography (MDCT). This was a retrospective study conducted on 511 patients (360 males and 151 female) referred for MDCT assessment of PNS over a two-year period. The mean age of our patients was 34.47 ± 10.69 years, aged between 18 and 79 years. Patients with nasal trauma, surgeries or any pathological diseases affecting the ethmoid roof were excluded from the study. Keros type II was the commonest presentation observed in 53.2% of cases, followed by type I in 12.5%, then type III in 11.7% of cases. Out of the 511 patients analyzed, 115 (22.5%) cas-

es had asymmetry (different types of OF) on both sides. Conclusion: The majority of studied Saudi adult population showed Keros type II (53.3%), followed by type I (12.5%). Keros type III was seen in 11.7% among the studied population.

Key words: Multidetector computed tomography – Endoscopic sinus surgery – Olfactory fossa – Keros classification

Abbreviations:

ESS, endoscopic sinus surgery
CT, computed tomography scan
OF, olfactory fossa
CREB, cribriform plate of ethmoid bone
LLCP, lateral lamella of cribriform plate
FE, Fovea ethmoidalis
MDCT, Multidetector Computed tomography
AEA, Anterior ethmoidal artery

INTRODUCTION

In the late 1980s, the endoscopic sinus surgery (ESS) was introduced as a new and best method for diagnosis and treatment of chronic rhinosinusitis through the open sinus surgery (Koele et al.,

Corresponding author: Wael Amin Nasr El-Din. Department of Human Anatomy and Embryology, Faculty of Medicine, Suez Canal University Ismailia, Egypt. Anatomy Department, Ibn Sina National College for Medical Studies, Jeddah, Saudi Arabia. Almahjar Street, 21418, Jeddah, Saudi Arabia. Phone: +966544384526; Fax: +9666262888
E-mail: waelamin2010@yahoo.com

Submitted: 23 November, 2019. Accepted: 9 January 2020.

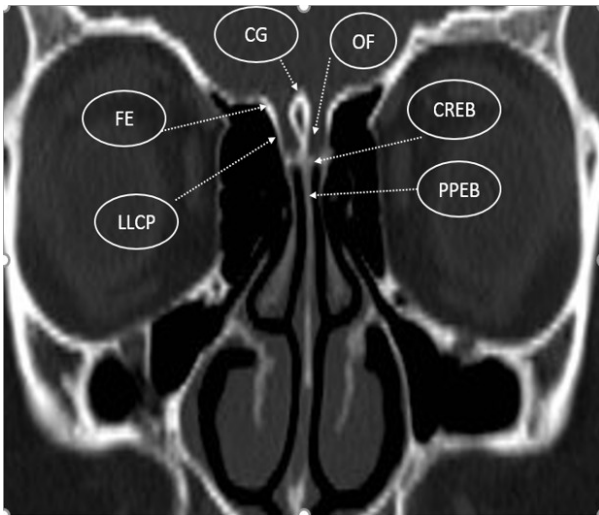


Fig 1. Coronal CT image showing; The different anatomical structures of the ethmoid roof; crista galli (CG), olfactory fossa (OF), fovea ethmoidalis (FE), lateral lamella of the cribriform plate (LLCP), perpendicular plate of ethmoid bone (PPEB), cribriform plate of ethmoid bone (CREB).

2002). The most known complications encountered during sinus surgeries are skull base entry, orbital and ocular injuries (McMains, 2008). The meticulous knowledge of the anatomy and anatomic variations, together with a preoperative computed tomography (CT) assessment, help us to pass safely through the paranasal sinus region in order to minimize the risk for the patient (Stankiewicz and Chow, 2004).

The ethmoid bone is one of the most complex structures of the base of the skull. The olfactory fossa (OF) is a small depression in the anterior cranial fossa, whose base is formed by the cribriform plate of the ethmoid bone (CPEB). This thin, perforated bone isolates the nasal cavity from the anterior cranial fossa. The lateral boundary of OF is formed by the lateral lamella of the cribriform plate (LLCP) and its medial is formed by crista galli (Jacob and Kaul, 2014). Olfactory bulbs and tracts are lodged in the fossa (Vaid and Vaid, 2015) (Fig. 1).

Fovea ethmoidalis (FE) is a part of the frontal bone, which shares as a part of the roof of the ethmoid bony labyrinth. It is the barrier between the ethmoidal air cells from the anterior cranial fossa. FE joins medially with LLCP, which is the thinnest bone in the anterior skull base and forms the lateral wall of the olfactory fossa (Arun et al., 2017; Stammberger and Kennedy, 1995). The angle at the junction between FE and LLCP determines the shape of the FE, as it may be straight or in the form of a broken wing if the angle increased (Terrier et al., 1995) (Fig. 1).

Anatomic variations in LLCP and asymmetry of FE or OF are considered as risk factors during functional ESS as they may lead to various injuries. Hence, preoperative assessment by CT is now compulsory before the functional ESS

(Cashman et al., 2011).

In 1962, Keros examined 450 skulls to study the relation between the OF and the ethmoid roof/FE. The depth of OF is measured by the vertical height of the LLCP, the difference between the height of the cribriform plate and ethmoid roof. He classified the depth of the OF into 3 categories: Keros I (26.3% of population), the depth is 1-3 mm, with short lateral lamella, and the ethmoid roof is almost in the same horizontal plane as the cribriform plate of ethmoid. In Keros II (73.3% of population), the depth is from 4 to 7, with longer lateral lamella. In Keros III (0.5% of population), the depth is 8–16 mm, and the ethmoid roof lies essentially higher than the cribriform plate (Som et al., 2011; Reddy and Dev, 2012; Keros, 1962). This study did not describe the measurements between 3 and 4 mm as well as between 7 and 8 mm.

Based on Keros classification, if the height of LLCP is increased, the risk of its iatrogenic damage is presumably increased. The thin LLCP is vulnerable to possible injury during surgery, trauma or tumor erosion in Keros type III (Ulualp, 2008)

The depth of the OF varies among various racial populations had been studied by many researches (Bista et al., 2010; Elwany et al., 2010; Soares et al., 2008), however no previous data considering this point of research was reported among Saudi population. Our study aimed to use coronal paranasal sinus CT scan imaging to measure the variations of the height of OF among Saudi adults. The study concentrated on measuring the height of the LLCP according to Keros classification.

MATERIALS AND METHODS

Study design

A morphometric, retrospective blinded study consisting of 511 subjects underwent multidetector computed tomography (MDCT) imaging of the nose and paranasal sinuses with a Phillips 64-slice CT machine (kVp (kilo voltage peak)=100, MAs (Milli-Ampere seconds)=200, rotation time=0.4 second, FOV (field of view)=240 mm, slice thickness=1 mm, reconstruction interval=0.3 mm, pitch=0.399; Philips, Australia) at Radio-diagnostic Department at Al-Jedaani Group Hospital in Jeddah, KSA. The study was conducted in the period between February 2017 and July 2019. Informed consent was obtained from all subjects, and ethical approval for this study was obtained from the Local Institutional Human Ethics Committee (IHEC# H-28-30042017).

360 (70.5%) males and 151 (29.5%) females were investigated. All subjects were Saudi adults aged between 18 to 79 years, who presented to the outpatient clinic with chronic symptoms attributed to the PNS and referred for MDCT. Subjects less than 18 years old, those with facial congenital anomalies, trauma or with pathology involv-

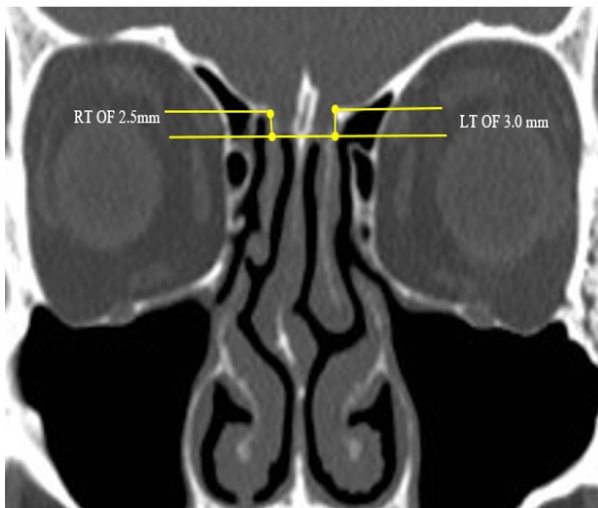


Fig 2. Coronal CT image showing bilateral Keros Type I olfactory fossae.

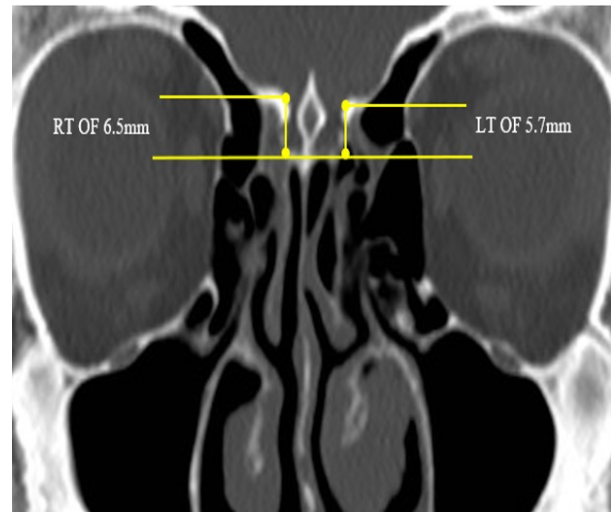


Fig 3. Coronal CT image showing bilateral Keros Type II olfactory fossae.

ing the ethmoidal roof including both olfactory fossae were excluded from this study.

Measurements

We utilized picture archiving and communication system (PACS) to assess the variations in the depth of OF, and then classify them based on Keros classification. Only coronal sections were examined in this study and the images were analyzed in the bone window and were interpreted by the same observer. The following anatomical landmarks were recognized and utilized for measurements.

1. FE (The medial ethmoidal roof point)
2. Cribriform plate of ethmoid bone
3. LLCP

Two horizontal lines were drawn; one at the level of FE point and the other at the level of the cribriform plate. The vertical height of LLCP was measured between these two horizontal lines using a single caliper with the smallest unit of measurement at 0.5mm. The meticulous depth of OF was determined according to modified Keros classification; measuring the vertical height of lateral lamella and was classified as follows: Keros I: OF is 1 to 3.99 mm deep, Keros II: OF is 4 to 7.99 mm deep, Keros III: OF is 8 to 16 mm deep.

Statistical analysis

The analysis was performed using a software

program (Statistical Package for Social Sciences SPSS version 20.0). All values were expressed as means \pm standard deviation (SD). Categorical variables were presented in number and percentage (%). Qualitative variables were correlated using Chi-Square test. Significance of the data was determined by P values, where a P value \leq 0.05 was considered to be significant.

RESULTS

MDCT scans of the 511 adult patients were included in this study. There were 360 (70.5%) males and 151 (29.5%) females. The ages of the patients ranged between 18 and 79 years with a mean of 34.47 ± 10.69 years.

In the present study both the right and left lateral lamellae in the CT scan were measured and coded separately. The measurements of the lateral lamella were simultaneously obtained using the distance-measuring tool (a single caliper with smallest unit of measurement at 0.5mm).

According to Keros classification, the OF of all subjects were distributed in such a way that type II was the commonest presentation observed in 53.2% of cases (Fig. 3), followed by type I in 12.5% of cases (Fig. 2) then type III in 11.7% of cases (Fig. 4) (Table 1).

As for gender, and based on Keros classification, the OF were compared between males and fe-

Table 1. Distribution of 511 olfactory fossae based on Keros classification according to gender

| Gender | Type I n (%) | Type II n (%) | Type III n (%) | Asymmetry n (%) | Total n (%) | X ² (P) |
|--------|-----------------|------------------|-------------------|--------------------|----------------|-----------------------|
| Male | 46 (12.8) | 186 (51.7) | 43 (11.9) | 85 (23.6) | 360 (70.5) | 1.326 (p = 0.7) |
| Female | 18 (11.9) | 86 (57) | 17 (11.3) | 30 (19.9) | 151 (29.5) | |
| Total | 64 (12.5) | 272 (53.3) | 60 (11.7) | 115 (22.5) | 511 (100) | |

n – number of the studied subjects; (%) – Percent; X² – chi square; P – probability value

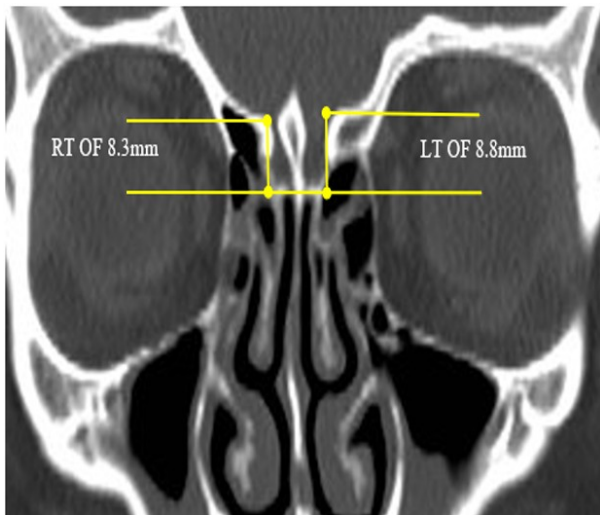


Fig 4. Coronal CT image showing bilateral Keros Type III olfactory fossae.

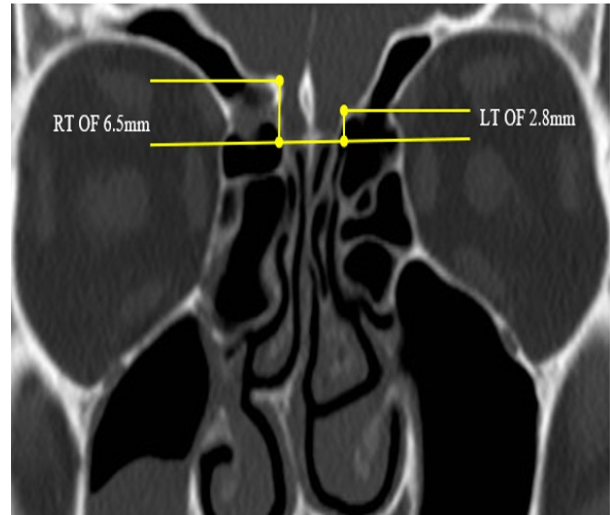


Fig 5. Coronal CT image showing asymmetry in configuration of both olfactory fossa; type II on right and type I on left side.

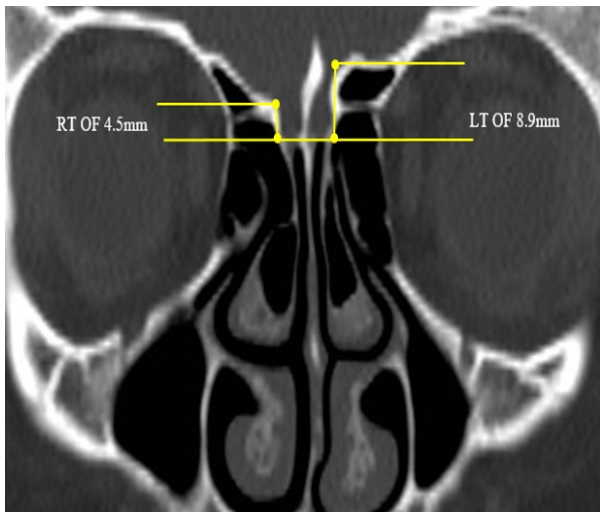


Fig 6. Coronal CT image showing asymmetry in configuration of both olfactory fossa; type II on right and type III on left side.

males. The most common type of the OF was Type II, which was observed in higher frequency in females than in males; followed by Type I, which was slightly more common in males than females; and then type III, with approximately the same prevalence in males and females. The previous results were statistically insignificant difference between both sexes (Table 1).

Regarding asymmetry, the incidence of different types of OF in the right and left sides was 22.5% of

cases. The prevalence was more common in males than females, with statistically insignificant difference between both sexes (Figs. 5,6) (Table 1).

When the right- and left-sided OF were compared out of 1022 sides, the most common type of OF in both sides was Type II, which was observed with almost similar prevalence (64.4 % in the right side versus 64.2% in the left one). Type I had a higher frequency in the left side as compared to the right (19.8% versus 16.6%), whereas Type III was more common in the right side (19.0%) if compared to the left one (16.1%). These results indicate a statistically insignificant difference in the distribution of Keros type between both sides ($p > 0.05$) (Table 2).

Comparing of OF regarding both sides and sex, and based on Keros classification, showed that: OF Keros type I was found among 16.7% of cases, type II among 64.7% and type III among 18.6% of cases on the right side among males. Type I was found among 16.6%, type II among 63.6% and type III among 19.9% on the right side in females. No statistically significant difference was found between males and females (Table 3). On the other hand, OF was Keros type I in 20.8%, type II in 61.9% and type III in 17.2% males on the left side. Similarly, among females on the left side, OF was Keros type I in 17.2%, type II in 69.5% and type III in 13.3%. There is no significant association be-

Table 2. Distribution of olfactory fossa based on Keros classification according to the side

| Side | Type I n (%) | Type II n (%) | Type III n (%) | X ² (P) |
|-------|-----------------|------------------|-------------------|-----------------------|
| Right | 85 (16.6) | 329 (64.4) | 97 (19.0) | 2.63 (p = 0.2) |
| Left | 101 (19.8) | 328 (64.2) | 82 (16.1) | |
| Total | 186 (18.2) | 657 (64.3) | 179 (17.5) | |

n – number of the studied subjects; (%) – Percent; X² – chi square; P – probability value

Table 3. Distribution of right OF based on Keros Classification according to gender

| Side | Type I n (%) | Type II n (%) | Type III n (%) | X ² (P) |
|--------|-----------------|------------------|-------------------|-----------------------|
| Male | 60 (16.7) | 233 (64.7) | 67 (18.6) | 0.11 (p = 0.9) |
| Female | 25 (16.6) | 96 (63.6) | 30 (19.9) | |
| Total | 85 (16.6) | 329 (64.4) | 97 (19.0) | |

OF – olfactory fossa; n – number of the studied subjects; (%) – Percent; X² – chi square; P – probability value

Table 4. Distribution of left OF based on Keros Classification according to gender

| Side | Type I n (%) | Type II n (%) | Type III n (%) | X ² (P) |
|--------|-----------------|------------------|-------------------|-----------------------|
| Male | 75 (20.8) | 223 (61.9) | 62 (17.2) | 2.71 (p = 0.2) |
| Female | 26 (17.2) | 105 (69.5) | 20 (13.3) | |
| Total | 101 (19.8) | 328 (64.2) | 82 (16.1) | |

OF – olfactory fossa; n – number of the studied subjects; (%) – Percent; X² – chi square; P – probability value

tween sex and Keros type on both right and left sides (Table 4).

DISCUSSION

CT scan of the nose and paranasal sinus plays a key role in pre-operative evaluation of patients undergoing ESS (Nair, 2012). The increase in dependence on the endoscopy in sinus evaluation and surgery made it very important for the surgeon to gain an excellent knowledge about the meticulous anatomy of the anterior skull base for each individual patient for pre-operative evaluation in order to avoid the possible complications that may occur during sinus surgery (Athamneh et al., 2015).

The present study observed Keros type II to be the commonest presentation, followed by type I and then type III. This is in agreement with the studies conducted by Nair (2012) among Indian population, Athamneh et al. (2015) among Jordanian population, Pawar et al. (2018) among Indian population, Souza et al. (2008) among Brazilian population, Elwany et al. (2010) among Egyptian population and Kaplanoglu et al. (2013) among Turkish population; all of which observed that type II is the commonest presentation, followed by type I and type III (Table 5). However, Floreani et al. (2006) and Nitinavakarn et al. (2005) reported type II as the commonest presentation, followed by type

III then type I (Table 5).

In contrast with our results, the studies performed by Paber et al. (2008) among Filipinos population, and Shama and Montaser (2015) among Egyptian population, demonstrated that the majority of studied subjects were classified as Keros type I, followed by type II and then type III (Table 5).

Asymmetry of the anterior skull base, and in particular in the ethmoid roof, is an important finding to be checked in the CT scan analysis before ESS (Kizilkaya et al., 2006). In the present study, asymmetry was found in 22.5% of our cases according to Keros classification. This matches closely with the results of Babu et al. (2018), who conducted a study among Indian population and reported that 21.7% of the studied subjects had asymmetry. However, in the study conducted by Pawar et al. (2018) among Indian population, asymmetry was found only in 11.5% of patients. Solares et al. (2008) reported asymmetry of the ethmoid roof in all subjects in an American study, and attributed their findings to the use of computer-aided CT scan analysis, which allowed more precise measurement.

Regarding gender, our study showed that Keros type II was the most common type in both males and females, follow by type I and then type III. 22.5% of the study group had asymmetry of the ethmoid roof (23.6% in males versus 19.9 % in females). However, the difference in between males and females was statistically insignificant ($p > 0.05$). In agreement with our study, Athamneh et al. (2015) conducted a study among Jordanian populations and found that type II was the most common type in both sexes, followed by type I and then type III. In contrast, Shama and Montaser (2015) conducted a study among Egyptian populations, and reported that type I was the most common type in females, while type II was the most common in male patients. Type III was the least

Table 5. Keros classification among different studies

| Author | Country | n= | Keros I (%) | Keros II (%) | Keros III (%) | Asymmetry (%) | | |
|---------------------|------------|-----|-------------|--------------|---------------|---------------|-----|----|
| Original (Keros) | Germany | 450 | 26.3 | 73.3 | 0.5 | 73.3 | 0.5 | -- |
| Present study | KSA | 511 | 12.5 | 53.2 | 11.7 | 22.5 | | |
| Nair | India | 180 | 17.2 | 77.2 | 5.6 | 11.7 | | |
| Athamneh et al. | Jordan | 100 | 22.0 | 70.5 | 7.5 | -- | | |
| Pawar et al. | India | 200 | 18.5 | 74.5 | 7.0 | 11.5 | | |
| Souza et al. | Brazil | 200 | 26.2 | 73.3 | 0.5 | 12.0 | | |
| Elwany et al. | Egypt | 300 | 42.5 | 56.8 | 0.6 | -- | | |
| Kaplanoglu et al. | Turkey | 500 | 13.4 | 76.1 | 10.5 | -- | | |
| Floreani et al. | Cadaveric | 22 | 23.0 | 50.0 | 27.0 | -- | | |
| Nitinavakarn et al. | Thailand | 88 | 11.9 | 68.8 | 19.3 | -- | | |
| Paber et al. | Philippine | 109 | 81.8 | 17.7 | 0.5 | -- | | |
| Shama and Montaser | Egypt | 100 | 56.5 | 40.5 | 3.0 | -- | | |

n – number of the studied subjects; (%) – Percent

Table 6. Keros classification according to gender among different studies

| Author | Country | n= | Keros I (%) | | Keros II (%) | | Keros III (%) | |
|---------------------------|-------------------|-----|-------------|------|--------------|------|---------------|------|
| | | | M | F | M | F | M | F |
| Present study | KSA | 511 | 12.8 | 11.9 | 51.7 | 57.0 | 11.9 | 11.3 |
| Athamneh et al. | Jordan | 100 | 20.0 | 25.0 | 70.0 | 70.0 | 9.2 | 5.0 |
| Shama and Montaser | Egypt | 100 | 47.0 | 66.0 | 48.0 | 33.0 | 5.0 | 1.0 |
| Paber et al. | Philippine | 109 | 74.5 | 87.0 | 24.5 | 12.1 | 1.0 | 0 |

n – number of the studied subjects; (%) – Percent; M – Males; F – females

Table 7. Keros classification according to side among different studies

| Author | Country | n= | Keros I (%) | | Keros II (%) | | Keros III (%) | |
|--------------------------|-------------------|-----|-------------|------|--------------|------|---------------|-------|
| | | | Right | Left | Right | Left | Right | Left |
| Present study | KSA | 511 | 16.6 | 19.8 | 64.4 | 64.2 | 19.0 | 16.01 |
| Athamneh et al. | Jordan | 100 | 23.0 | 21.0 | 70.0 | 70.0 | 6.0 | 9.0 |
| Pawar et al. | India | 200 | 22.0 | 15.0 | 72.0 | 77.0 | 6.0 | 8.0 |
| Kaplanoglu et al. | Turkey | 500 | 13.6 | 13.2 | 76.2 | 76.2 | 10.2 | 10.8 |
| Paber et al. | Philippine | 109 | 79.8 | 83.5 | 20.2 | 15.6 | 0 | 0.9 |
| Elwany et al. | Egypt | 300 | 41.3 | 43.7 | 58.0 | 55.7 | 0.6 | 0.6 |

n – number of the studied subjects; (%) – Percent

common type in both sexes (Table 6). Paber et al. (2008) conducted a study among Filipino patients, and found that type I was the most common type in both sexes, followed by type II. Only one male was classified as Keros III, and no females were found in this type. The distribution of Keros classification between males and females was significantly different ($p = 0.01$) (Table 6).

In our work, asymmetric cases were more common in males than in females (23.6% versus 19.9%). This is in agreement with findings of a study reported by Reiß and Reiß (2011), in which there were more asymmetric cases in males than females (38% versus 29%) and the difference was statistically significant. Moreover, Elwany et al. (2010) reported that asymmetric cases in males are more frequent than in females (11% versus 2%).

Regarding laterality, and out of 511 patients (1022 sides), the most common type in both sides is type II; type I is more common in the left side, while type III is more common in the right side. Athamneh et al. (2015), Pawar et al. (2018) and Kaplanoglu et al. (2013) reported that the most common type in both sides is type II; type I is more common in the right side, while type III is more common in the left side (Table 7). Paber et al. (2008) investigated the Filipino patients and showed that the most common type in both sides was type I, followed by type II. Only (0.9%) was Keros III for the left lateral lamella, but was absent for the right (Table 7). Elwany et al. (2010) found that the most common type in both sides is type II; type I is more common in the left side, while type III is equal in both sides (Table 7).

In the present study, there was a statistically in-

significant difference in the Keros classification of the right and left lateral lamellae. In contrast, the study performed by Jacob et al. (2014) in cadaveric skulls of Indian population showed a statistically significant difference in the distribution of Keros types between the right and left sides. Zacharek et al. (2005) and Lebowitz et al. (2001) had demonstrated in their studies that the ethmoid roof is significantly lower in the right side as compared to the left one. Reiß and Reiß (2011) conducted a study among 644 German patients, and found that 221 (31%) of cases had asymmetry between the height of the ethmoid roof on the right and left sides. Of these 221, 160 (72.4%) were lower on the right side, whereas 61 (27.6%) were lower on the left.

Gera et al. (2018) measured the angle between LLCPC and the continuation of a horizontal plane passing through the cribriform plate and suggested a new classification, (Gera classification), based on the measured angle and on the presumptive risk of iatrogenic injuries. Class I (the angle $>80^\circ$ with low risk), class II (the angle is from 45° to 80° with medium risk) and class III (the angle $<45^\circ$ with high risk). Preti et al. (2018) reported that Gera classification might be more sensitive and specific in detecting a potential LLCPC damage, which may lead to cerebrospinal fluid leak during ESS, together with the Keros classification, are beneficial in the preoperative CT scan assessment.

Recently, Abdullah et al. (2019) proposed that the anterior ethmoidal artery (AEA) may be injured during ESS due to its proximity at the skull base. More caution should be taken in the existence of a long LLCPC because AEA will run freely below the base of the skull.

These wide ranges of variations in all previous

measurements regarding the asymmetry, gender or laterality among various populations may be attributed to genetic or ethnic causes. Moreover, the number of studied subjects, method of measurements and even the standardization of Keros classifications may play a major role in these variations.

Conclusion: The present study demonstrated that the majority of Saudi population showed Keros type II (53.2%), followed by type I (12.5%) and then type III (11.7%). Comprehension of these variations after CT scan imaging are crucial before ESS and for ENT surgeons in the operation theater to avoid critical expected complications.

REFERENCES

- ABDULLAH B, LIM EH, HUSAIN S, SNIDVONGS K, WANG Y (2019) Anatomical variations of anterior ethmoidal artery and their significance in endoscopic sinus surgery: a systematic review. *Surg Radiol Anat*, 41 (5): 491-499.
- ARUN G, MOIDEEN SP, MOHAN M, AFROZE MKH, THAMPY AS (2017) Anatomical variations in superior attachment of uncinate process and localization of frontal sinus outflow tract. *Int J Otorhinolaryngol Head Neck Surg*, 3(2): 176-179.
- ATHAMNEH I, HAZAIMEH B, SHAWAQFEH J, HANI MB, ALTAMIMI A (2015) Keros classification among Jordanian population. *JRMS*, 22(3): 69-72.
- BABU AC, NAIR MRPB, KURIAKOSE AM (2018) Olfactory fossa depth: CT analysis of 1200 patients. *Indian J Radiol Imaging*, 28(4): 395-400.
- BASAK S, AKDILLI A, KARAMAN CZ, KUNT T (2005) Assessment of some important anatomical variations and variations and dangerous areas of the paranasal sinuses by computed tomography in children. *Int J Pediatr Otorhinolaryngol*, 55(2): 81-89.
- BISTA M, MAHARJAN M, KAFLE P, SHRESTHA S, KC T (2010) Computed tomographic assessment of lateral lamella of cribriform plate and comparison of depth of olfactory fossa. *JNMA J Nepal Med Assoc*, 49(178): 92-95.
- CASHMAN EC, MACMAHON PJ, SMYTH D (2011) Computed tomography scans of paranasal sinuses before functional endoscopic sinus surgery. *World J Radiol*, 3(8): 199-204.
- ELWANY S, MEDANNI A, EID M, ALY A, EL-DALY A, AMMAR SR (2010) Radiological observations on the olfactory fossa and ethmoid roof. *J Laryngol Otol*, 124 (12): 1251-1256.
- FLOREANI SR, NAIR SB, SWITAJEWSKI MC, WORMALD PJ (2006) Endoscopic anterior ethmoidal artery ligation: a cadaver study. *Laryngoscope*, 116(7): 1263-1267.
- GERA R, MOZZANICA F, KARLIGKIOTIS A, PRETI A, BANDI F, GALLO S, SCHINDLER A, BULGHERONI C, OTTAVIANI F, CASTELNUOVO P (2018) Lateral lamella of the cribriform plate, a keystone landmark: proposal for a novel classification system. *Rhinology*, 56(1): 65-72.
- JACOB TG, KAUL JM (2014) Morphology of the olfactory fossa – A new look. *J Anat Soc India*, 63(1): 30-35.
- KAPLANOGLU H, KAPLANOGLU V, DILLI A, TOPRAK U, HEKIMOĞLU B (2013) An analysis of the anatomic variations of the paranasal sinuses and ethmoid roof using computed tomography. *Eurasian J Med*, 45(2): 115-125.
- KEROS P (1962) On the practical value of differences in the level of the lamina cribrosa of the ethmoid. *Z Laryngol Rhinol Otol*, 41: 809-813.
- KIZILKAYA E, KANTARCI M, CINAR BASEKIM C, MUTLU H, KARAMAN B, DANE S, OKUR A, SEKMENLI N (2006) Asymmetry of the height of the ethmoid roof in relationship to handedness. *Laterality*, 11 (4): 297-303.
- KOELE W, STAMMBERGER H, LACKNER A, REITNER P (2002) Image guided surgery of paranasal sinuses and anterior skull base—five years experience with the Insta Trak-System. *Rhinology*, 40(1): 1-9.
- LEBOWITZ RA, TERK A, JACOB JB, HOLIDAY RA (2001) Asymmetry of the ethmoid roof, analysis using coronal computed tomography. *Laryngoscope*, 111 (12): 2122-2124.
- MCMAINS KC (2008) Safety in endoscopic sinus surgery. *Curr Opin Otolaryngol Head Neck Surg*, 16(3): 247-251.
- NAIR S (2012) Importance of ethmoidal roof in endoscopic sinus surgery. *Open access Sci Rep*, 1: 251.
- NITINAVAKARN B, THANAVIRATANANICH S, SANGSILP N (2005) Anatomical variations of the lateral nasal wall and paranasal sinuses: a CT study for endoscopic sinus surgery (ESS) in Thai patients. *J Med Assoc Thai*, 88(6): 763-768.
- PABER JELB, CABATO MSD, VILLARTA RL, HERNANDEZ JG (2008) Radiographic analysis of the ethmoid roof based on Keros classification among Filipinos. *Philipp J Otolaryngol Head Neck Surg*, 23(1): 15-19.
- PAWAR A, KONDE S, BHOLE P (2018) Assessment of depth of olfactory fossa in pre-functional endoscopic sinus surgery computed tomography scan of paranasal sinuses. *Int J Otorhinolaryngol Head Neck Surg*, 4 (1): 83-86.
- PRETI A, MOZZANICA F, GERA R, GALLO S, ZOCCHI J, BANDI F, GUIDUGLI G, AMBROGI F, YAKIREVITCH A, SCHINDLER A, DRAGONETTI A, CASTELNUOVO P, OTTAVIANI F (2018) Horizontal lateral lamella as a risk factor for iatrogenic cerebrospinal fluid leak. Clinical retrospective evaluation of 24 cases. *Rhinology*, 56(4): 358-363.
- REDDY UD, DEV B (2012) Pictorial essay: Anatomical variations of paranasal sinuses on multidetector computed tomography – How does it help FESS surgeons? *Indian J Radiol Imaging*, 22(4): 317-324.
- REIß M, REIß G (2011) Height of right and left ethmoid roofs: aspects of laterality in 644 patients. *Int J Otolaryngol*, 2011: 508907.
- SHAMA SAM, MONTASER M (2015) Variations of the height of the ethmoid roof among Egyptian adult popu-

lation. *EJRN*, 46: 929-936.

STAMMBERGER HR, KENNEDY DW (1995) Paranasal sinuses: anatomic terminology and nomenclature. *Ann Otol Rhinol Laryngol Suppl*, 167: 7-16.

STANKIEWICZ JA, CHOW JM (2004) The low skull base: an invitation to disaster. *Am J Rhinol*, 18(1): 35-40.

SOLARES CA, LEE WT, BATRA PS, CITARDI MJ (2008) Lateral lamella of the cribriform plate. Software-enabled computed tomographic analysis and its clinical relevance in skull base surgery. *Arch Otolaryngol Head Neck Surg*, 134(3): 285-289.

SOM PM, LAWSON W, FATTERPEKAR GM, ZINREICH J (2011) Embryology, Anatomy, Physiology and imaging of the sinonasal cavities. *Head Neck Imag*, 5: 119-128.

SOUZA SA, SOUZA MMA, IDAGAWA M, WOLOSKER AMB, AJZEN SA (2008) Computed tomography assessment of the ethmoid roof: a relevant region at risk in endoscopic sinus surgery. *Radiol Bras*, 41(3): 143-147.

TERRIER F, WEBER W, RUEFENACHT D, PORCELLINI B (1995) Anatomy of the ethmoid: CT, endoscopic, and macroscopic. *AJR Am J Roentgenol*, 144(3): 493-500.

ULUALP SO (2008) Complications of endoscopic sinus surgery: appropriate management of complications. *Curr Opin Otolaryngol Head Neck Surg*, 16(3): 252-259.

VAID S, VAID N (2015) Normal anatomy and anatomic variants of the paranasal sinuses on computed tomography. *Neuroimaging Clin N Am*, 25(4): 527-548.

ZACHAREK MA, HAN JK, ALLEN R, WEISSMAN JL, HWANG PH (2005) Sagittal and coronal dimensions of the ethmoid roof: a radioanatomic study. *Am J Rhinol*, 19(4): 348-352.